

Cite as: E. A. Stadtmauer *et al.*, *Science*
10.1126/science.aba7365 (2020).

CRISPR-engineered T cells in patients with refractory cancer

Edward A. Stadtmauer,^{1,2*†} Joseph A. Fraietta,^{2,3,4,5*} Megan M. Davis,^{5,6} Adam D. Cohen,^{1,2} Kristy L. Weber,^{2,7} Eric Lancaster,⁸ Patricia A. Mangan,¹ Irina Kulikovskaya,⁵ Minnal Gupta,⁵ Fang Chen,⁵ Lifeng Tian,⁵ Vanessa E. Gonzalez,⁵ Jun Xu,⁵ In-young Jung,^{4,5} J. Joseph Melenhorst,^{3,5,6} Gabriela Plesa,⁵ Joanne Shea,⁵ Tina Matlawski,⁵ Amanda Cervini,⁵ Avery L. Gaymon,⁵ Stephanie Desjardins,⁵ Anne Lamontagne,⁵ January Salas-Mckee,⁵ Andrew Fesnak,^{5,6} Donald L. Siegel,^{5,6} Bruce L. Levine,^{5,6} Julie K. Jadlowsky,⁵ Regina M. Young,⁵ Anne Chew,⁵ Wei-Ting Hwang,⁹ Elizabeth O. Hexner,^{1,2} Beatriz M. Carreno,^{3,5,6} Christopher L. Nobles,⁴ Frederic D. Bushman,⁴ Kevin R. Parker,¹⁰ Yanyan Qi,¹¹ Ansuman T. Satpathy,^{10,11} Howard Y. Chang,^{10,12} Yangbing Zhao,^{5,6} Simon F. Lacey,^{5,6*} Carl H. June^{2,3,5,6*†}

¹Division of Hematology-Oncology, Department of Medicine, Perelman School of Medicine, University of Pennsylvania, Philadelphia, PA, USA. ²Abramson Cancer Center, Perelman School of Medicine, University of Pennsylvania, Philadelphia, PA, USA. ³Parker Institute for Cancer Immunotherapy, Perelman School of Medicine, University of Pennsylvania, Philadelphia, PA, USA. ⁴Department of Microbiology, Perelman School of Medicine, University of Pennsylvania, Philadelphia, PA, USA. ⁵Center for Cellular Immunotherapies, Perelman School of Medicine, University of Pennsylvania, Philadelphia, PA, USA. ⁶Department of Pathology and Laboratory Medicine, Perelman School of Medicine, University of Pennsylvania, Philadelphia, PA, USA. ⁷Department of Orthopaedic Surgery, Perelman School of Medicine, University of Pennsylvania, Philadelphia, PA, USA. ⁸Department of Neurology, Perelman School of Medicine, University of Pennsylvania, Philadelphia, PA, USA. ⁹Department of Biostatistics, Epidemiology and Informatics, Perelman School of Medicine, University of Pennsylvania, Philadelphia, PA, USA. ¹⁰Center for Personal Dynamic Regulomes, Stanford University School of Medicine, Stanford, CA, USA. ¹¹Department of Pathology, Stanford University School of Medicine, Stanford, CA, USA. ¹²Howard Hughes Medical Institute, Stanford University School of Medicine, Stanford, CA, USA.

*These authors contributed equally to this work. †Corresponding author. Email: edward.stadtmauer@pennmedicine.upenn.edu (E.A.S.); cjune@upenn.edu (C.H.J.)

CRISPR-Cas9 gene editing provides a powerful tool to enhance the natural ability of human T cells to fight cancer. We report a first-in-human phase I clinical trial to test the safety and feasibility of multiplex CRISPR-Cas9 editing to engineer T cells in three patients with refractory cancer. Two genes encoding the endogenous T cell receptor (TCR) chains, TCR α (*TRAC*) and TCR β (*TRBC*) were deleted in T cells to reduce TCR mispairing and to enhance the expression of a synthetic, cancer-specific TCR transgene (NY-ESO-1). Removal of a third gene encoding PD-1 (*PDCDI*), was performed to improve anti-tumor immunity. Adoptive transfer of engineered T cells into patients resulted in durable engraftment with edits at all three genomic loci. Though chromosomal translocations were detected, the frequency decreased over time. Modified T cells persisted for up to 9 months suggesting that immunogenicity is minimal under these conditions and demonstrating the feasibility of CRISPR gene-editing for cancer immunotherapy.

Gene editing offers the potential to correct DNA mutations, and may offer promise to treat or eliminate countless human genetic diseases. The goal of gene editing is to change the DNA of cells with single base pair precision. The principle was first demonstrated in mammalian cells when it was shown that expression of a rare cutting endonuclease to create double-strand DNA breaks resulted in repair by homologous and non-homologous recombination (1). A variety of engineered nucleases were then developed to increase efficiency and enable potential therapeutic applications, including zinc finger nucleases, homing endonucleases, transcription activator-like effector nucleases and CRISPR-Cas9 (clustered regularly interspaced short palindromic repeats associated with Cas9 endonuclease) (2). The first pilot human trials using genome editing were conducted in patients with HIV/AIDS and targeted the white blood cell protein *CCR5*, with the goal of mutating the gene by non-homologous recombination and thereby inducing resistance

to HIV infection (3, 4). The incorporation of multiple guide sequences in CRISPR-Cas9 permits, in principle, multiplex genome engineering at several sites within a mammalian genome (5–9). The ability of CRISPR to facilitate efficient multiplex genome editing has greatly expanded the scope of possible targeted genetic manipulations, enabling new possibilities such as simultaneous deletion or insertion of multiple DNA sequences in a single round of mutagenesis. The prospect of using CRISPR-engineering to treat a host of diseases such as inherited blood disorders and blindness is moving closer to reality.

Recent advances in CRISPR-Cas9 technology have also permitted efficient DNA modifications in human T cells, which holds great promise for enhancing the efficacy of cancer therapy. T lymphocytes are specialized immune cells that are largely at the core of the modern day cancer immunotherapy revolution. The T cell receptor (TCR) complex is located on the surface of T cells, and is central for initiating

successful anti-tumor responses by recognizing foreign antigens/peptides bound to MHC-molecules. One of the most promising areas of cancer immunotherapy involves adoptive cell therapy, where the patient's own T cells are genetically engineered to express a synthetic (transgenic) TCR that can specifically detect and kill tumor cells. Recent studies have shown safety and promising efficacy of such adoptive T cell transfer approaches using transgenic TCRs specific for the immunogenic NY-ESO-1 tumor antigen in patients with myeloma, melanoma and sarcoma (10–12). One limitation of this approach is that the transgenic TCR has been shown to mispair and/or compete for expression with the alpha and beta chains of the endogenous TCR (13–15). Mispairing of the therapeutic TCR alpha and beta chains with endogenous alpha and beta chains reduces therapeutic TCR cell surface expression and potentially generates self-reactive TCRs.

A further shortcoming of adoptively transferred T cells has been the induction of T cell dysfunction or exhaustion leading to reduced efficacy (16). PD-1-deficient allogeneic mouse T cells with transgenic TCRs showed enhanced responses to alloantigens, indicating that the PD-1 protein on T cells plays a negative regulatory role in antigen responses that are likely to be cell intrinsic (17). The adoptive transfer of PD-1 deficient T cells in mice with chronic lymphocytic choriomeningitis virus infection initially leads to enhanced cytotoxicity and later to enhanced accumulation of terminally differentiated T cells (18). Antibody blockade of PD-1, or disruption/knockdown of the gene encoding PD-1 (i.e., *PDCDI*), improved chimeric antigen receptor (CAR) or TCR T cell-mediated killing of tumor cells in vitro and enhanced clearance of PD-L1⁺ tumor xenografts in vivo (19–23). In preclinical studies, we and others found that CRISPR-Cas9-mediated disruption of *PDCDI* in human T cells transduced with a CAR increased anti-tumor efficacy in tumor xenografts (24–26). Adoptive transfer of transgenic TCR T cells specific for the cancer antigen NY-ESO-1, in combination with a monoclonal antibody targeting PD-1, enhanced antitumor efficacy in mice (27). We therefore designed a first-in-human, phase I human clinical trial to test the safety and feasibility of multiplex CRISPR-Cas9 genome editing for a synthetic biology cancer immunotherapy application. We chose to target endogenous *TRAC*, *TRBC* and *PDCDI* on T cells to increase the safety and efficacy profile of NY-ESO-1 TCR-expressing engineered cells. In principle, this strategy allowed us to increase exogenous TCR expression and reduce the potential for mixed heterodimer formation (i.e., by deleting the alpha and beta TCR domain genes *TRAC* and *TRBC* respectively), and to limit the development of T cell exhaustion which can be triggered by the checkpoint ligands PD-L1 and PD-L2 (i.e., by deleting *PDCDI*).

Results

Clinical protocol

The phase I human trial (ClinicalTrials.gov NCT03399448) was designed to assess the safety and feasibility of infusing autologous NY-ESO-1 TCR engineered T cells in patients after CRISPR-Cas9 editing of the *TRAC*, *TRBC* and *PDCDI* loci. During the manufacturing process, cells were taken out of the cancer patient, engineered and then infused back into the individual. The genetically-engineered T cell product was termed “NYCE” (NY-ESO-1 transduced CRISPR 3X edited cells) and is referred to as NYCE hereafter. During clinical development of the protocol, we elected to use a TCR rather than a CAR because the incidence of cytokine release syndrome is generally less prevalent using TCRs (11). In principle, this allowed a more discriminating assessment of whether gene editing with Cas9 was potentially immunogenic or toxic when compared with the baseline low level of adverse events observed in our previous clinical trial targeting NY-ESO-1 with transgenic TCRs (11). The autologous T cells were engineered by lentiviral transduction to express an HLA-A2*0201-restricted TCR-specific for the SLLMWITQC peptide in NY-ESO-1 and LAGE-1. The manufacturing process, vector design and clinical protocol for NYCE T cells are described in the materials and methods section and are depicted schematically (figs. S1 and S2). Of the six patients that were initially enrolled, four patients had successfully engineered T cells that were subjected to detailed release criteria testing as specified in the FDA accepted Investigational New Drug (IND) application (table S1). See fig. S3 for the consort diagram. Of the four patients with cell products available, one patient assigned with unique patient number (UPN) 27 experienced rapid clinical progression and was no longer eligible for infusion due to the inability to meet protocol mandated safety criteria (see supplementary materials). Of the three patients that were infused with CRISPR-Cas9 engineered T cells, two patients had refractory advanced myeloma and one patient had a refractory metastatic sarcoma not responding to multiple prior therapies (Table 1). The patients were given lymphodepleting chemotherapy with cyclophosphamide and fludarabine on days -5 to -3 (i.e., prior to administration with CRISPR-Cas9 engineered T cells) and a single infusion of 1×10^8 manufactured CRISPR-Cas9 engineered T cells per kg on day 0 of the protocol (fig. S2). No cytokines were administered to the patients.

Characteristics of infused CRISPR-Cas9-engineered T cell products

The T cell product was manufactured by electroporation of ribonucleoprotein complexes (RNP) comprising recombinant Cas9 loaded with equimolar mixtures of sgRNA for *TRAC*, *TRBC* and *PDCDI* followed by lentiviral transduction of the transgenic TCR (Fig. 1A). All products were expanded to

$>1 \times 10^{10}$ T cells by the time of harvest (Fig. 1B). The transgenic TCR could be detected by flow cytometric staining for V β 8.1 or dextramer staining, ranging from 2 – 7% of T cells in the final product (Fig. 1C). The frequency of editing as determined by digital PCR varied according to the sgRNA and was approximately 45% for *TRAC*, 15% for *TRBC* and 20% for *PDCDI* (Fig. 1D). Final product transduction efficiency, CD4:CD8 ratio, and dosing are shown in table S2.

The potency of the final engineered T cells were assessed by co-culture with HLA-A2⁺ tumor cells engineered to express NY-ESO-1 (Fig. 2A). The engineered T cells had potent antigen-specific cytotoxicity over a wide range of effector to target cell ratios. Interestingly, the cells treated with CRISPR-Cas9 were more cytotoxic than control cells transduced with the TCR but electroporated without CRISPR-Cas9 (i.e., cells that retained endogenous TCR). This is consistent with previous findings in mouse T cells, when a transgenic TCR was inserted into the endogenous locus, ablating expression of the endogenous TCR (15). Further studies will be required to determine if PD-1 knockout contributes to the increased potency afforded by knockout of the endogenous TCR.

We developed a sensitive immunoassay for detection of *Streptococcus pyogenes* Cas9 protein and quantified Cas9 early in the manufacturing process, showing declining levels that were <0.75 fg/cell in the harvested final product (Fig. 2C). Using a competitive fluorescence ELISA screen, we found that healthy donors have humoral reactivity to Cas9 in serum (Fig. 2D) and T cells (Fig. 2E), confirming previous reports (28–30). Interestingly, we found that the three patients tested at a variety of time points after infusion of the engineered T cells did not develop humoral responses to Cas9. The lack of immunization to Cas9 is consistent with the extended persistence of the infused cells (Fig. 3) and could be a consequence of the low content of Cas9 in the infused product and/or to the immunodeficiency in the patients due to their extensive previous treatment histories (Table 1).

Engraftment and persistence of infused CRISPR-Cas9-engineered T cells in cancer patients

Three patients with advanced, refractory cancer were given infusions of the CRISPR-Cas9 engineered T cells. The infusions were well-tolerated with no serious adverse events (Table 2); importantly there were no cases of cytokine release syndrome, which is a potentially life threatening systemic inflammatory response that has been associated with cancer immunotherapies (31). All three patients were infused with 1×10^8 cells/kg, and due to the considerable variation in TCR transduction efficiencies (table S2), the absolute number of infused engineered T cells ranged from 6.0×10^7 to 7.1×10^8 cells. Despite the variation in engineered cells, there were high peak levels and sustained persistence of the engineered cells in the blood of all three patients (Fig. 3A). The peak and

steady state level of engineered cells was lowest in patient UPN35, who also had the lowest transduction efficiency (table S2). The persistence of the transduced cells is remarkably stable from three to nine months after infusion, varying from 5 to 50 cells per μ l of blood (Fig. 3B). Using a subject-specific piecewise linear model, the decay half-life in days of the transduced cells was 20.3, 121.8 and 293.5 for UPN07, UPN35, and UPN39. The average decay half-life was 83.9 days (15–153, 95% CI) for the three subjects as estimated by a piecewise linear mixed effects model that assumes cells decay linearly from day 14 post-expansion and random effects to allow varying level of expansion (or peak values) across subjects. The stable engraftment of our engineered T cells is remarkably different from previously reported trials with NY-ESO-1 engineered T cells, where the half-life of the cells in blood was \sim 1 week (11, 32, 33). Biopsy specimens of bone marrow in the myeloma patients and tumor in the sarcoma patient demonstrated trafficking of the engineered T cells to the tumor in all three patients at levels approaching those in the blood compartment (Fig. 3A).

To determine the engraftment frequency of the CRISPR-Cas9 gene-edited cells, we initially used chip-based digital PCR. With this assay, engraftment of cells with editing at the *TRAC* and *PDCDI* locus was evident in all three patients (Fig. 3C). There was sustained persistence of *TRAC* and *PDCDI* edits in patient UPN39 and UPN07 at frequencies of 5 to 10% of circulating peripheral blood mononuclear cells (PBMC), while *TRBC* edited cells were lowest in frequency and only transiently detected. The low-level engraftment of *TRBC* edited cells is likely related to the observation that this locus had the lowest level of editing efficiency in our preclinical studies (25), and in the harvested products (Fig. 1D).

Analysis of the fidelity of CRISPR-Cas9 genome editing

On- and off-target editing efficiency was assessed in the NYCE cells at the end of product manufacturing. Details of the analysis for UPN07 are shown as an example in Fig. 4, with detailed analysis of the other three manufactured products shown in the table S3. The average on-target CRISPR-Cas9 editing efficiency for all engineered T cell products for each target is shown in Table 3. We used iGUIDE (34), a modification of the GUIDE-seq method (35), to analyze the Cas9-mediated cleavage specificity. A complication of assays to assess repair by non-homologous end joining (NHEJ) is that DNA double-strand breaks are formed spontaneously during cell division at high rates in the absence of added nucleases (36), which can increase the background in assays of off-target cleavage. The distribution of on-target and off-target cleavage is expected to vary for the three sgRNAs that were used in the manufacturing process (fig. S1A). Of the three sgRNA, there were more off-target mutations identified for *TRBC* than for the other loci (Fig. 4C and figs. S4 and S5). The sgRNA for

PDCDI was the most specific, as very few off-target edits were identified in over 7000 sites of cleavage, and there were very few off-target reads identified at the *TRAC1* and *TRAC2* loci (Fig. 4C).

The genomic localization of identified DNA cleavage sites was as expected, given the chromosomal location of the three targeted genes on chromosomes 2, 7 and 14 (Fig. 4A). The distribution of the incorporation of the dsODN label around on-target sites, based on pileups within a window of 100 base pairs, is shown in Fig. 4B and fig. S4. While most mutations were on target, there were off-target mutations identified (Fig. 4C and fig. S5). For the *TRAC* sgRNA, there were low abundance mutations within the transcriptional unit of *CLIC2* (chloride intracellular channel 2); however disruption of *CLIC2* in T cells is not expected to have negative consequences since it is not reported to be expressed in T cells. For the *TRBC* sgRNA, off-target edits were identified in genes encoding a transcriptional regulator (*ZNF609*) and a long intergenic non-protein coding RNA (*LINC00377*) (table S3). In addition to the above post-hoc investigations of multiplex editing specificity, all products were shown not to have cellular transformation by virtue of the absence of long-term growth prior to infusion (table S1).

Detection of chromosomal translocations in CRISPR-Cas9 engineered T cells

In addition to the above detection of repair of double-strand DNA breaks by NHEJ, on-target mutagenesis by engineered nucleases can result in deletions, duplications, inversions, and translocations, and can also lead to complex chromosomal rearrangements under some conditions (37). CRISPR-Cas9 has been used to intentionally create oncogenic chromosomal rearrangements (38). In preclinical studies with human T cells, simultaneous gene editing of *TRAC* and *CD52* using transcription activator-like effector nucleases (TALENs) led to translocations that were detected at frequencies of 10^{-4} to 10^{-2} (39). In a subsequent clinical report using dual-gene editing with TALENs, chromosomal rearrangements were observed in 4% of infused cells (40). In order to study the safety and genotoxicity of multiplex CRISPR-Cas9 genome editing on three chromosomes, we employed stringent release criteria of the manufactured cells and assays to detect translocations (fig. S6). We developed and qualified qPCR assays to quantify the 12 potential translocations that could occur with the simultaneous editing of four loci: *TRAC*, *TRBC1*, *TRBC2*, *PDCDI* (see materials and methods). We observed translocations in all manufactured products, however the translocations were at the limit of detection for the assay in patient UPN39 (Fig. 5A). *TRBC1:TRBC2* was the most abundant rearrangement (Fig. 5A), resulting in a 9.3 kB deletion (supplementary materials). The deletion and translocations peaked on days 5 to 7 of manufacturing and then

declined in frequency until cell harvest. The translocations and the *TRBC1:TRBC2* deletion were evident in the three patients between 10 days after infusion and 30 to 170 days after infusion (Fig. 5B). However, the rearrangements declined in frequency in vivo suggesting that they conferred no evidence of a growth advantage over many generations of expansion in the patients on this trial (Fig. 3, A and B). At day 30, 150 and 170 in patients UPN07, UPN35 and UPN39, chromosomal translocations were at the limits of detection or not detected for all rearrangements except for the 9.3 kB deletion for *TRBC1:TRBC2*.

Single-cell RNA sequencing analysis reveals evolution of CRISPR-Cas9 engineered NYCE cells

We used single cell RNA sequencing (scRNAseq) to comprehensively characterize the transcriptomic phenotype of the NYCE T cells and their evolution over time in patient UPN39 (fig. S7). UPN39 was chosen because they had the highest level of cell engraftment and because this patient had evidence of tumor regression. CRISPR-Cas9 engineered T cells were infused to patient UPN39 and recovered after infusion from the blood on day 10 (D10) and at ~4 months (day, D113) and were analyzed by scRNAseq, as described in the materials and methods. For each sample (infusion product, D10 and D113), T cells were sorted based on expression of CD4 or CD8 and processed using droplet-based 5' scRNAseq. From the gene expression libraries, PCR was used to further amplify cellular cDNA corresponding to the NY-ESO-1 TCR transgene, as well as *TRAC*, *TRBC* and *PDCDI* target sequences, allowing us to genotype single cells as wild-type or mutant. In the infusion product, cells were identified that contained mutations in all three target sequences (Fig. 6, A and B). The most commonly mutated gene was *TRAC*. Approximately 30% of cells had no mutations identified, while ~40% had 1 mutation, and ~20% and ~10% of the T cells in the manufactured product were double-mutated and triple-mutated respectively at the target sequences. Of the transgenic TCR⁺ cells in the infusion product, monogenic mutations were less frequent than di-genic and tri-genic mutations (Fig. 6A). Single-cell genotyping of UPN39 cells at 10 days and 4 months after infusion showed a decline in the frequency of gene-edited T cells from the levels in the infusion product, and this decline occurred regardless of whether the cells were transduced with the NY-ESO-1 TCR (Fig. 6C). The frequency of gene-edited cells was quite stable between day 10 and 4 months post-infusion, and remarkably, approximately 40% of the peripheral blood circulating T cells in this patient 4 months after infusion were mutated at any one of the targeted genes (Fig. 6, B and C, and table S4).

Of particular interest is the frequency and evolution of PD-1 deficient T cells due to the previous mention that genetic disruption of *PDCDI* in CAR and TCR T cells enhances

antitumor efficacy in preclinical models (19, 21–24). We found that ~25% of the T cells expressing the NY-ESO-1 TCR in the infusion product had mutations in the *PDCDI* locus (fig. S8). It is interesting that the frequency of cells with edits in the *PDCDI* locus decreased to ~5% of the cells expressing the transgenic TCR at 4 months after infusion. This would be consistent with mouse studies of chronic infection where PD-1 deficient T cells are less able to establish memory (18).

Figure 6D shows the distribution of engineered T cells in patients expressing the NY-ESO-1 TCR transgene over time, as they evolved from the infusion product at baseline and then again at 4 months in vivo. In the heat map (Fig. 6E), the most differentially expressed genes in the cells expressing the NY-ESO-1 transcript at the various time points are shown in table S5. It is notable that this patient had increases in expression of genes associated with central memory (*IL7R*, *TCF7*) over time (Fig. 6, D and E, and table S4). This is in marked contrast to the recently published results with NY-ESO-1 T cells in the absence of genome editing, where the infused transgenic T cells evolved to a terminally differentiated phenotype and displayed characteristics of T cell exhaustion in cancer patients (12).

Clinical observations

The clinical course of the three infused cancer patients is shown in Fig. 7 (and described in the supplementary materials and methods). No patient experienced cytokine release syndrome or overt side effects attributed to the cell infusion (table S5). The best clinical responses were stable disease in two patients. UPN39 had a mixed response with a ~50% decrease in a large abdominal mass that was sustained for four months (Fig. 7D), although other lesions progressed. As of December 2019, all patients have progressed: two are receiving other therapies and UPN07 died from progressive myeloma.

Biopsies of bone marrow and tumor showed trafficking of the NYCE engineered T cells to the sites of tumor in all three patients (Fig. 3A). It is interesting to note that even though the tumor biopsies revealed residual tumor, in both patients with myeloma there was a reduction in the target antigens NY-ESO-1 and/or LAGE-1 (fig. S9). The reduction of target antigen was transient in patient UPN07 and persistent in patient UPN35. This result is consistent with an on-target effect of the infused cells, likely resulting in tumor editing (41).

To determine whether the NYCE cells retained antitumor activity after infusion, samples of blood obtained from patients 3 to 9 months after infusion were expanded in culture in the presence of NY ESO-1 peptide and assessed for cytotoxicity against tumor cells (Fig. 7E and fig. S10). Antigen-specific cytotoxicity was observed in all three patients. It is interesting to note that the most potent anti-tumor cytotoxicity was observed in UPN39, as UPN39 was the only patient to have tumor regression after infusion of the CRISPR-Cas9

engineered T cells (Fig. 7D).

Discussion

Our phase I first-in-human pilot study demonstrates the initial safety and feasibility of multiplex CRISPR-Cas9 T cell human genome engineering in patients with advanced, refractory cancer. In one patient analyzed at depth, a frequency of 30% of di-genic and tri-genic editing was achieved in the infused cell population, and 20% of the TCR transgenic T cells in circulation 4 months later had persisting di-genic and tri-genic edits. We chose to redirect specificity of the T cells with a T cell receptor, rather than a chimeric antigen receptor, in order to avoid the chimeric antigen receptor-associated potential toxicities such as cytokine release syndrome (31). This provided a lower baseline toxicity profile, thus enhancing the ability to detect toxicity specifically associated with the CRISPR-Cas9 engineering process. We observed mild toxicity and most of the adverse events were attributed to the lymphodepleting chemotherapy. We note that while the initial clinical results have acceptable safety, experience with more patients given infusions of CRISPR-engineered T cells with higher editing efficiencies, and longer observation after infusion, will be required to fully assess the safety of this approach.

Our large-scale product manufacturing process resulted in gene editing efficiencies similar to our preclinical studies (24). A surprising finding was the high-level engraftment and long-term persistence of the infused CRISPR-Cas9 engineered T cells. In previous clinical studies testing adoptively transferred NY-ESO-1 transgenic T cells, the engrafted cells and had an initial decay half-life of approximately 1 week (10–12). The explanation for the extended survival that we observed remains to be determined, and could include the editing of the endogenous TCR, PD-1 and/or the choice of the TCR and vector design.

The use of scRNAseq technology permitted the analysis of the transcriptome of the infused NY-ESO-1 specific T cells (i.e., CRISPR-Cas9 engineered T cells) at baseline and for up to four months in vivo. The results shown for UPN39 revealed that the infused cells evolved to a state consistent with central memory. These results are in contrast to a recent study where the infused NY-ESO-1 T cells evolved to a state consistent with T cell exhaustion (12). A limitation of our in vivo single cell analysis is that for purposes of feasibility, it is limited to the one patient who had the highest level of engraftment. Another limitation is that we were not able to compare the transcriptional state of the modified cells in the tumor microenvironment to circulating NYCE T cells.

Analysis of the manufacturing process in vitro demonstrated monochromosomal translocations and rearrangements, and some of these persisted in vivo. The translocations were not random in occurrence and occurred most frequently

between *PDCDI:TRAC* and *TRBC1:TRBC2*. The frequency of translocations that we observed with tri-genic editing is similar to that reported for di-genic editing using transcription activator-like effector nuclease (TALEN)-mediated gene editing in preclinical and clinical studies, where rearrangements were detected in approximately 4% of cells (39, 40). It is important to note that healthy individuals often harbor oncogenic translocations in B and T cells (42–44). T cells bearing translocations can persist for months to years without evidence of pathogenicity (45–47).

Antagonism of the PD-1:PD-L1 costimulatory pathway can result in organ-specific and systemic autoimmunity (17, 48). PD-1 has been reported to function as a haploinsufficient tumor suppressor in mouse T cells (49). Our patients have had engraftment with PD-1 deficient T cells and to date, there is no evidence of autoimmunity or T cell genotoxicity.

In conclusion, our phase I human pilot study has confirmed that multiplex CRISPR-Cas9 editing of the human genome is possible at clinical scale. We note that while the initial clinical results are safe, experience with more patients given infusions with higher editing efficiencies and longer observation after infusion will be required to fully assess the safety of this approach. The potential rejection of infused cells due to pre-existing immune responses to Cas9 (28, 29) does not appear to be a barrier to the application of this promising technology. Finally, it is important to note that our manufacturing was based on the reagents available in 2016, when our protocol had been reviewed by the NIH Recombinant DNA Advisory Committee and received approval. Our Investigational New Drug Application was subsequently reviewed and accepted by the U.S. FDA. There has been rapid progress in the field since that time, with the development of reagents that should increase efficiencies and decrease off-target editing using CRISPR-based technology (50).

Materials and methods summary

Experimental design

The clinical protocol is listed at [trial ClinicalTrials.gov](http://clinicaltrials.gov) NCT03399448. Protocol #1604-1524 “Phase I Trial of Autologous T Cells Engineered to Express NY-ESO-1 TCR and Gene Edited to Eliminate Endogenous TCR and PD-1” was reviewed and approved by the U.S. National Institutes of Health Recombinant DNA Advisory Committee on June 21, 2016. See fig. S1B for clinical trial design. Patient demographics are shown in Table 1. A list of adverse events is depicted in Table 2.

Guide RNAs (gRNA)

The genomic gRNA target sequences with PAM in bold were: *TRAC1* and *TRAC2*: 5'-TG TGCTAGACATGAGGTCTAT**GG-3'**, *TRBC*: 5'-GGAGAATGACGAGTGGACCC**AGG-3'**, and *PDCDI*: 5'-GGCGCCTGGCCAGTCGTCT**GGG-3**. *In vitro* transcribed

gRNA was prepared from linearized DNA (Aldevron) using Bulk T7 Megascript 5X (Ambion) and purified using RNeasy Maxi Kit (Qiagen).

Recombinant Cas9 protein

Cas9 recombinant protein derived from *Streptococcus pyogenes* was TrueCut Cas9 v2 (Catalogue # A36499, ThermoFisher). Cas9 RNP was made by incubating protein with gRNA at a molar ratio of 1:1 at 25°C for 10 minutes immediately prior to electroporation.

Lentiviral vector manufacturing

The 8F TCR recognizes the HLA-A*0201 SLLMWITQC epitope on NY-ESO-1 and LAGE-1. The 8F TCR was isolated from a T cell clone obtained from patient after vaccination with NY-ESO-1 peptide. The TCR sequences were cloned into a transfer plasmid that contains the EF-1 α promoter, a cPPT sequence, a rev response element and a woodchuck hepatitis virus posttranscriptional regulatory element (WPPE) as shown in fig. S1B. Plasmid DNA was manufactured at PureSyn, Inc. Lentiviral vector was produced at the University of Pennsylvania Center for Advanced Retinal and Ocular Therapeutics using transient transfection with four plasmids expressing the transfer vector, Rev, VSV-G and gag/pol, in 293T cells.

REFERENCES AND NOTES

1. P. Rouet, F. Smih, M. Jasin, Introduction of double-strand breaks into the genome of mouse cells by expression of a rare-cutting endonuclease. *Mol. Cell. Biol.* **14**, 8096–8106 (1994). doi:10.1128/MCB.14.12.8096 Medline
2. M. H. Porteus, A new class of medicines through DNA editing. *N. Engl. J. Med.* **380**, 947–959 (2019). doi:10.1056/NEJMra1800729 Medline
3. P. Tebas, D. Stein, W. W. Tang, I. Frank, S. Q. Wang, G. Lee, S. K. Spratt, R. T. Surosky, M. A. Giedlin, G. Nichol, M. C. Holmes, P. D. Gregory, D. G. Ando, M. Kalos, R. G. Collman, G. Binder-Scholl, G. Plesa, W.-T. Hwang, B. L. Levine, C. H. June, Gene editing of *CCR5* in autologous CD4 T cells of persons infected with HIV. *N. Engl. J. Med.* **370**, 901–910 (2014). doi:10.1056/NEJMoa1300662 Medline
4. L. Xu, J. Wang, Y. Liu, L. Xie, B. Su, D. Mou, L. Wang, T. Liu, X. Wang, B. Zhang, L. Zhao, L. Hu, H. Ning, Y. Zhang, K. Deng, L. Liu, X. Lu, T. Zhang, J. Xu, C. Li, H. Wu, H. Deng, H. Chen, CRISPR-edited stem cells in a patient with HIV and acute lymphocytic leukemia. *N. Engl. J. Med.* **381**, 1240–1247 (2019). doi:10.1056/NEJMoa1817426 Medline
5. M. Jinek, K. Chylinski, I. Fonfara, M. Hauer, J. A. Doudna, E. Charpentier, A programmable dual-RNA-guided DNA endonuclease in adaptive bacterial immunity. *Science* **337**, 816–821 (2012). doi:10.1126/science.1225829 Medline
6. L. Cong, F. A. Ran, D. Cox, S. Lin, R. Barretto, N. Habib, P. D. Hsu, X. Wu, W. Jiang, L. A. Marraffini, F. Zhang, Multiplex genome engineering using CRISPR/Cas systems. *Science* **339**, 819–823 (2013). doi:10.1126/science.1231143 Medline
7. P. K. Mandal, L. M. R. Ferreira, R. Collins, T. B. Meissner, C. L. Boutwell, M. Friesen, V. Vrbanac, B. S. Garrison, A. Stortchevoi, D. Bryder, K. Musunuru, H. Brand, A. M. Tager, T. M. Allen, M. E. Talkowski, D. J. Rossi, C. A. Cowan, Efficient ablation of genes in human hematopoietic stem and effector cells using CRISPR/Cas9. *Cell Stem Cell* **15**, 643–652 (2014). doi:10.1016/j.stem.2014.10.004 Medline
8. J. F. Hultquist, J. Hiatt, K. Schumann, M. J. McGregor, T. L. Roth, P. Haas, J. A. Doudna, A. Marson, N. J. Krogan, CRISPR-Cas9 genome engineering of primary CD4⁺ T cells for the interrogation of HIV-host factor interactions. *Nat. Protoc.* **14**, 1–27 (2019). doi:10.1038/s41596-018-0069-7 Medline
9. R. O. Bak, D. P. Dever, A. Reinisch, D. Cruz Hernandez, R. Majeti, M. H. Porteus,

- Multiplexed genetic engineering of human hematopoietic stem and progenitor cells using CRISPR/Cas9 and AAV6. *eLife* **6**, e27873 (2017). [doi:10.7554/eLife.27873](https://doi.org/10.7554/eLife.27873) [Medline](#)
10. P. F. Robbins, R. A. Morgan, S. A. Feldman, J. C. Yang, R. M. Sherry, M. E. Dudley, J. R. Wunderlich, A. V. Nahvi, L. J. Helman, C. L. Mackall, U. S. Kammula, M. S. Hughes, N. P. Restifo, M. Raffeld, C.-C. R. Lee, C. L. Levy, Y. F. Li, M. El-Gamil, S. L. Schwarz, C. Laurencot, S. A. Rosenberg, Tumor regression in patients with metastatic synovial cell sarcoma and melanoma using genetically engineered lymphocytes reactive with NY-ESO-1. *J. Clin. Oncol.* **29**, 917–924 (2011). [doi:10.1200/JCO.2010.32.2537](https://doi.org/10.1200/JCO.2010.32.2537) [Medline](#)
 11. A. P. Rapoport, E. A. Stadtmauer, G. K. Binder-Scholl, O. Goloubeva, D. T. Vogl, S. F. Lacey, A. Z. Badros, A. Garfall, B. Weiss, J. Finklestein, I. Kulikovskaya, S. K. Sinha, S. Kronsberg, M. Gupta, S. Bond, L. Melchiori, J. E. Brewer, A. D. Bennett, A. B. Gerry, N. J. Pumphrey, D. Williams, H. K. Tayton-Martin, L. Ribeiro, T. Holdich, S. Yanovich, N. Hardy, J. Yared, N. Kerr, S. Philip, S. Westphal, D. L. Siegel, B. L. Levine, B. K. Jakobsen, M. Kalos, C. H. June, NY-ESO-1-specific TCR-engineered T cells mediate sustained antigen-specific antitumor effects in myeloma. *Nat. Med.* **21**, 914–921 (2015). [doi:10.1038/nm.3910](https://doi.org/10.1038/nm.3910) [Medline](#)
 12. T. S. Nowicki, B. Berent-Maoz, G. Cheung-Lau, R. R. Huang, X. Wang, J. Tsoi, P. Kaplan-Lefko, P. Cabrera, J. Tran, J. Pang, M. Macabali, I. P. Garcilazo, I. B. Carretero, A. Kalbasi, A. J. Cochran, C. S. Grasso, S. Hu-Lieskovan, B. Chmielowski, B. Comin-Anduj, A. Singh, A. Ribas, A pilot trial of the combination of transgenic NY-ESO-1-reactive adoptive cellular therapy with dendritic cell vaccination with or without ipilimumab. *Clin. Cancer Res.* **25**, 2096–2108 (2019). [doi:10.1158/1078-0432.CCR-18-3496](https://doi.org/10.1158/1078-0432.CCR-18-3496) [Medline](#)
 13. E. Provasi, P. Genovese, A. Lombardo, Z. Magnani, P.-Q. Liu, A. Reik, V. Chu, D. E. Paschon, L. Zhang, J. Kuball, B. Camisa, A. Bondanza, G. Casorati, M. Ponzoni, F. Ciceri, C. Bordignon, P. D. Greenberg, M. C. Holmes, P. D. Gregory, L. Naldini, C. Bonini, Editing T cell specificity towards leukemia by zinc finger nucleases and lentiviral gene transfer. *Nat. Med.* **18**, 807–815 (2012). [doi:10.1038/nm.2700](https://doi.org/10.1038/nm.2700) [Medline](#)
 14. G. M. Bendle, C. Linnemann, A. I. Hooijkaas, L. Bies, M. A. de Witte, A. Jorritsma, A. D. M. Kaiser, N. Pouw, R. Debets, E. Kieback, W. Uckert, J.-Y. Song, J. B. A. G. Haanen, T. N. M. Schumacher, Lethal graft-versus-host disease in mouse models of T cell receptor gene therapy. *Nat. Med.* **16**, 565–570, 1p, 570 (2010). [doi:10.1038/nm.2128](https://doi.org/10.1038/nm.2128) [Medline](#)
 15. K. Schober, T. R. Müller, F. Gökmén, S. Grassmann, M. Effenberger, M. Poltorak, C. Stemmerger, K. Schumann, T. L. Roth, A. Marson, D. H. Busch, Orthotopic replacement of T-cell receptor α - and β -chains with preservation of near-physiological T-cell function. *Nat. Biomed. Eng.* **3**, 974–984 (2019). [doi:10.1038/s41551-019-0409-0](https://doi.org/10.1038/s41551-019-0409-0) [Medline](#)
 16. A. Schietinger, J. J. Delrow, R. S. Basom, J. N. Blattman, P. D. Greenberg, Rescued tolerant CD8 T cells are preprogrammed to reestablish the tolerant state. *Science* **335**, 723–727 (2012). [doi:10.1126/science.1214277](https://doi.org/10.1126/science.1214277) [Medline](#)
 17. H. Nishimura, M. Nose, H. Hiai, N. Minato, T. Honjo, Development of lupus-like autoimmune diseases by disruption of the PD-1 gene encoding an ITIM motif-carrying immunoreceptor. *Immunity* **11**, 141–151 (1999). [doi:10.1016/S1074-7613\(00\)80089-8](https://doi.org/10.1016/S1074-7613(00)80089-8) [Medline](#)
 18. P. M. Odorizzi, K. E. Pauken, M. A. Paley, A. Sharpe, E. J. Wherry, Genetic absence of PD-1 promotes accumulation of terminally differentiated exhausted CD8⁺ T cells. *J. Exp. Med.* **212**, 1125–1137 (2015). [doi:10.1084/jem.20142237](https://doi.org/10.1084/jem.20142237) [Medline](#)
 19. L. J. Rupp, K. Schumann, K. T. Roybal, R. E. Gate, C. J. Ye, W. A. Lim, A. Marson, CRISPR/Cas9-mediated PD-1 disruption enhances anti-tumor efficacy of human chimeric antigen receptor T cells. *Sci. Rep.* **7**, 737 (2017). [doi:10.1038/s41598-017-00462-8](https://doi.org/10.1038/s41598-017-00462-8) [Medline](#)
 20. I. Serganova, E. Moroz, I. Cohen, M. Moroz, M. Mane, J. Zurita, L. Shenker, V. Ponomarev, R. Blasberg, Enhancement of PSMA-directed CAR adoptive immunotherapy by PD-1/PD-L1 blockade. *Mol. Ther. Oncolytics* **4**, 41–54 (2016). [doi:10.1016/j.omto.2016.11.005](https://doi.org/10.1016/j.omto.2016.11.005) [Medline](#)
 21. S. Su, B. Hu, J. Shao, B. Shen, J. Du, Y. Du, J. Zhou, L. Yu, L. Zhang, F. Chen, H. Sha, L. Cheng, F. Meng, Z. Zou, X. Huang, B. Liu, CRISPR-Cas9 mediated efficient PD-1 disruption on human primary T cells from cancer patients. *Sci. Rep.* **6**, 20070 (2016). [doi:10.1038/srep20070](https://doi.org/10.1038/srep20070) [Medline](#)
 22. L. Menger, A. Sledzinska, K. Bergerhoff, F. A. Vargas, J. Smith, L. Poirot, M. Pule, J. Hererro, K. S. Peggs, S. A. Quezada, TALEN-mediated inactivation of PD-1 in tumor-reactive lymphocytes promotes intratumoral T-cell persistence and rejection of established tumors. *Cancer Res.* **76**, 2087–2093 (2016). [doi:10.1158/0008-5472.CAN-15-3352](https://doi.org/10.1158/0008-5472.CAN-15-3352) [Medline](#)
 23. L. Cherkassky, A. Morello, J. Villena-Vargas, Y. Feng, D. S. Dimitrov, D. R. Jones, M. Sadelain, P. S. Adusumilli, Human CAR T cells with cell-intrinsic PD-1 checkpoint blockade resist tumor-mediated inhibition. *J. Clin. Invest.* **126**, 3130–3144 (2016). [doi:10.1172/JCI83092](https://doi.org/10.1172/JCI83092) [Medline](#)
 24. J. Ren, X. Liu, C. Fang, S. Jiang, C. H. June, Y. Zhao, Multiplex genome editing to generate universal CAR T cells resistant to PD1 inhibition. *Clin. Cancer Res.* **23**, 2255–2266 (2017). [doi:10.1158/1078-0432.CCR-16-1300](https://doi.org/10.1158/1078-0432.CCR-16-1300) [Medline](#)
 25. J. Ren, X. Zhang, X. Liu, C. Fang, S. Jiang, C. H. June, Y. Zhao, A versatile system for rapid multiplex genome-edited CAR T cell generation. *Oncotarget* **8**, 17002–17011 (2017). [doi:10.18632/oncotarget.15218](https://doi.org/10.18632/oncotarget.15218) [Medline](#)
 26. X. Liu, Y. Zhang, C. Cheng, A. W. Cheng, X. Zhang, N. Li, C. Xia, X. Wei, X. Liu, H. Wang, CRISPR-Cas9-mediated multiplex gene editing in CAR-T cells. *Cell Res.* **27**, 154–157 (2017). [doi:10.1038/cr.2016.142](https://doi.org/10.1038/cr.2016.142) [Medline](#)
 27. E. K. Moon, R. Ranganathan, E. Eruslanov, S. Kim, K. Newick, S. O'Brien, A. Lo, X. Liu, Y. Zhao, S. M. Albelda, Blockade of programmed death 1 augments the ability of human T cells engineered to target NY-ESO-1 to control tumor growth after adoptive transfer. *Clin. Cancer Res.* **22**, 436–447 (2016). [doi:10.1158/1078-0432.CCR-15-1070](https://doi.org/10.1158/1078-0432.CCR-15-1070) [Medline](#)
 28. C. T. Charlesworth, P. S. Deshpande, D. P. Dever, J. Camarena, V. T. Lemgart, M. K. Cromer, C. A. Vakulskas, M. A. Collingwood, L. Zhang, N. M. Bode, M. A. Behlke, B. Dejene, B. Cieniewicz, R. Romano, B. J. Lesch, N. Gomez-Ospina, S. Mantri, M. Pavel-Dinu, K. I. Weinberg, M. H. Porteus, Identification of preexisting adaptive immunity to Cas9 proteins in humans. *Nat. Med.* **25**, 249–254 (2019). [doi:10.1038/s41591-018-0326-x](https://doi.org/10.1038/s41591-018-0326-x) [Medline](#)
 29. D. L. Wagner, L. Amini, D. J. Wendering, L.-M. Burkhardt, L. Akyüz, P. Reinke, H.-D. Volk, M. Schmuck-Henneresse, High prevalence of *Streptococcus pyogenes* Cas9-reactive T cells within the adult human population. *Nat. Med.* **25**, 242–248 (2019). [doi:10.1038/s41591-018-0204-6](https://doi.org/10.1038/s41591-018-0204-6) [Medline](#)
 30. V. L. Simhadri, J. McGill, S. McMahon, J. Wang, H. Jiang, Z. E. Sauna, Prevalence of pre-existing antibodies to CRISPR-associated nuclease Cas9 in the USA population. *Mol. Ther. Methods Clin. Dev.* **10**, 105–112 (2018). [doi:10.1016/j.omtm.2018.06.006](https://doi.org/10.1016/j.omtm.2018.06.006) [Medline](#)
 31. D. T. Teachey, S. F. Lacey, P. A. Shaw, J. J. Melenhorst, S. L. Maude, N. Frey, E. Pequignot, V. E. Gonzalez, F. Chen, J. Finklestein, D. M. Barrett, S. L. Weiss, J. C. Fitzgerald, R. A. Berg, R. Aplenc, C. Callahan, S. R. Rheingold, Z. Zheng, S. Rose-John, J. C. White, F. Nazimuddin, G. Wertheim, B. L. Levine, C. H. June, D. L. Porter, S. A. Grupp, Identification of predictive biomarkers for cytokine release syndrome after chimeric antigen receptor T-cell therapy for acute lymphoblastic leukemia. *Cancer Discov.* **6**, 664–679 (2016). [doi:10.1158/2159-8290.CD-16-0040](https://doi.org/10.1158/2159-8290.CD-16-0040) [Medline](#)
 32. P. F. Robbins, S. H. Kassim, T. L. N. Tran, J. S. Crystal, R. A. Morgan, S. A. Feldman, J. C. Yang, M. E. Dudley, J. R. Wunderlich, R. M. Sherry, U. S. Kammula, M. S. Hughes, N. P. Restifo, M. Raffeld, C.-C. R. Lee, Y. F. Li, M. El-Gamil, S. A. Rosenberg, A pilot trial using lymphocytes genetically engineered with an NY-ESO-1-reactive T-cell receptor: Long-term follow-up and correlates with response. *Clin. Cancer Res.* **21**, 1019–1027 (2015). [doi:10.1158/1078-0432.CCR-14-2708](https://doi.org/10.1158/1078-0432.CCR-14-2708) [Medline](#)
 33. S. P. D'Angelo, L. Melchiori, M. S. Merchant, D. Bernstein, J. Glod, R. Kaplan, S. Grupp, W. D. Tap, K. Chagin, G. K. Binder, S. Basu, D. E. Lowther, R. Wang, N. Bath, A. Tipping, G. Betts, I. Ramachandran, J.-M. Navenot, H. Zhang, D. K. Wells, E. Van Winkle, G. Kari, T. Trivedi, T. Holdich, L. Pandite, R. Amado, C. L. Mackall, Antitumor activity associated with prolonged persistence of adoptively transferred NY-ESO-1^{259T} cells in synovial sarcoma. *Cancer Discov.* **8**, 944–957 (2018). [doi:10.1158/2159-8290.CD-17-1417](https://doi.org/10.1158/2159-8290.CD-17-1417) [Medline](#)
 34. C. L. Nobles, S. Reddy, J. Salas-McKee, X. Liu, C. H. June, J. J. Melenhorst, M. M. Davis, Y. Zhao, F. D. Bushman, iGUIDE: An improved pipeline for analyzing CRISPR cleavage specificity. *Genome Biol.* **20**, 14 (2019). [doi:10.1186/s13059-019-1625-3](https://doi.org/10.1186/s13059-019-1625-3) [Medline](#)
 35. S. Q. Tsai, Z. Zheng, N. T. Nguyen, M. Liebers, V. V. Topkar, V. Thapar, N. Wyvekens, C. Khayter, A. J. Iafrate, L. P. Le, M. J. Aryee, J. K. Joung, GUIDE-seq enables genome-wide profiling of off-target cleavage by CRISPR-Cas nucleases. *Nat. Biotechnol.* **33**, 187–197 (2015). [doi:10.1038/nbt.3117](https://doi.org/10.1038/nbt.3117) [Medline](#)
 36. M. M. Vilenchik, A. G. Knudson, Endogenous DNA double-strand breaks: Production, fidelity of repair, and induction of cancer. *Proc. Natl. Acad. Sci. U.S.A.*

- 100, 12871–12876 (2003). [doi:10.1073/pnas.2135498100](https://doi.org/10.1073/pnas.2135498100) [Medline](#)
37. M. Kosicki, K. Tomberg, A. Bradley, Repair of double-strand breaks induced by CRISPR-Cas9 leads to large deletions and complex rearrangements. *Nat. Biotechnol.* **36**, 765–771 (2018). [doi:10.1038/nbt.4192](https://doi.org/10.1038/nbt.4192) [Medline](#)
 38. D. Maddalo, E. Manchado, C. P. Concepcion, C. Bonetti, J. A. Vidigal, Y.-C. Han, P. Ogrodowski, A. Crippa, N. Rekhman, E. de Stanchina, S. W. Lowe, A. Ventura, In vivo engineering of oncogenic chromosomal rearrangements with the CRISPR/Cas9 system. *Nature* **516**, 423–427 (2014). [doi:10.1038/nature13902](https://doi.org/10.1038/nature13902) [Medline](#)
 39. L. Poirot, B. Philip, C. Schiffer-Mannioui, D. Le Clerre, I. Chion-Sotinel, S. Derniame, P. Potrel, C. Bas, L. Lemaire, R. Galetto, C. Lebuhotel, J. Eyquem, G. W.-K. Cheung, A. Duclert, A. Gouble, S. Arnould, K. Peggs, M. Pule, A. M. Scharenberg, J. Smith, Multiplex genome-edited T-cell manufacturing platform for “off-the-shelf” adoptive T-cell immunotherapies. *Cancer Res.* **75**, 3853–3864 (2015). [doi:10.1158/0008-5472.CAN-14-3321](https://doi.org/10.1158/0008-5472.CAN-14-3321) [Medline](#)
 40. W. Qasim, H. Zhan, S. Samarasinghe, S. Adams, P. Amrolia, S. Stafford, K. Butler, C. Rivat, G. Wright, K. Somana, S. Ghorashian, D. Pinner, G. Ahsan, K. Gilmour, G. Lucchini, S. Ingloft, W. Mifsud, R. Chiesa, K. S. Peggs, L. Chan, F. Farzeneh, A. J. Thrasher, A. Vora, M. Pule, P. Veys, Molecular remission of infant B-ALL after infusion of universal TALEN gene-edited CAR T cells. *Sci. Transl. Med.* **9**, eaaj2013 (2017). [doi:10.1126/scitranslmed.aaj2013](https://doi.org/10.1126/scitranslmed.aaj2013) [Medline](#)
 41. G. P. Dunn, A. T. Bruce, H. Ikeda, L. J. Old, R. D. Schreiber, Cancer immunoeediting: From immunosurveillance to tumor escape. *Nat. Immunol.* **3**, 991–998 (2002). [doi:10.1038/nri102-991](https://doi.org/10.1038/nri102-991) [Medline](#)
 42. J. Bäsecke, F. Griesinger, L. Trümper, G. Brittinger, Leukemia- and lymphoma-associated genetic aberrations in healthy individuals. *Ann. Hematol.* **81**, 64–75 (2002). [doi:10.1007/s00277-002-0427-x](https://doi.org/10.1007/s00277-002-0427-x) [Medline](#)
 43. S. I. Ismail, R. G. Naffa, A. M. Yousef, M. T. Ghanim, Incidence of bcr-abl fusion transcripts in healthy individuals. *Mol. Med. Rep.* **9**, 1271–1276 (2014). [doi:10.3892/mmr.2014.1951](https://doi.org/10.3892/mmr.2014.1951) [Medline](#)
 44. R. Chiarle, Translocations in normal B cells and cancers: Insights from new technical approaches. *Adv. Immunol.* **117**, 39–71 (2013). [doi:10.1016/B978-0-12-410524-9.00002-5](https://doi.org/10.1016/B978-0-12-410524-9.00002-5) [Medline](#)
 45. C. A. Michie, A. McLean, C. Alcock, P. C. Beverley, Lifespan of human lymphocyte subsets defined by CD45 isoforms. *Nature* **360**, 264–265 (1992). [doi:10.1038/360264a0](https://doi.org/10.1038/360264a0) [Medline](#)
 46. A. R. McLean, C. A. Michie, In vivo estimates of division and death rates of human T lymphocytes. *Proc. Natl. Acad. Sci. U.S.A.* **92**, 3707–3711 (1995). [doi:10.1073/pnas.92.9.3707](https://doi.org/10.1073/pnas.92.9.3707) [Medline](#)
 47. K. George, L. J. Chappell, F. A. Cucinotta, Persistence of space radiation induced cytogenetic damage in the blood lymphocytes of astronauts. *Mutat. Res.* **701**, 75–79 (2010). [doi:10.1016/j.mrgentox.2010.02.007](https://doi.org/10.1016/j.mrgentox.2010.02.007) [Medline](#)
 48. C. H. June, J. T. Warshauer, J. A. Bluestone, Is autoimmunity the Achilles' heel of cancer immunotherapy? *Nat. Med.* **23**, 540–547 (2017). [doi:10.1038/nm.4321](https://doi.org/10.1038/nm.4321) [Medline](#)
 49. T. Wartewig, Z. Kurgyis, S. Keppler, K. Pechloff, E. Hameister, R. Öllinger, R. Maresch, T. Buch, K. Steiger, C. Winter, R. Rad, J. Ruland, PD-1 is a haploinsufficient suppressor of T cell lymphomagenesis. *Nature* **552**, 121–125 (2017). [doi:10.1038/nature24649](https://doi.org/10.1038/nature24649) [Medline](#)
 50. C. A. Vakulskas, D. P. Dever, G. R. Rettig, R. Turk, A. M. Jacobi, M. A. Collingwood, N. M. Bode, M. S. McNeill, S. Yan, J. Camarena, C. M. Lee, S. H. Park, V. Wiebking, R. O. Bak, N. Gomez-Ospina, M. Pavel-Dinu, W. Sun, G. Bao, M. H. Porteus, M. A. Behlke, A high-fidelity Cas9 mutant delivered as a ribonucleoprotein complex enables efficient gene editing in human hematopoietic stem and progenitor cells. *Nat. Med.* **24**, 1216–1224 (2018). [doi:10.1038/s41591-018-0137-0](https://doi.org/10.1038/s41591-018-0137-0) [Medline](#)
 51. Y. Zhao, Z. Zheng, P. F. Robbins, H. T. Khong, S. A. Rosenberg, R. A. Morgan, Primary human lymphocytes transduced with NY-ESO-1 antigen-specific TCR genes recognize and kill diverse human tumor cell lines. *J. Immunol.* **174**, 4415–4423 (2005). [doi:10.4049/jimmunol.174.7.4415](https://doi.org/10.4049/jimmunol.174.7.4415) [Medline](#)
 52. S. Bownds, P. Tong-On, S. A. Rosenberg, M. Parkhurst, Induction of tumor-reactive cytotoxic T-lymphocytes using a peptide from NY-ESO-1 modified at the carboxy-terminus to enhance HLA-A2.1 binding affinity and stability in solution. *J. Immunother.* **24**, 1–9 (2001). [doi:10.1097/00002371-200101000-00001](https://doi.org/10.1097/00002371-200101000-00001) [Medline](#)
 53. Y. Zhao, A. D. Bennett, Z. Zheng, Q. J. Wang, P. F. Robbins, L. Y. L. Yu, Y. Li, P. E. Molloy, S. M. Dunn, B. K. Jakobsen, S. A. Rosenberg, R. A. Morgan, High-affinity TCRs generated by phage display provide CD4⁺ T cells with the ability to recognize and kill tumor cell lines. *J. Immunol.* **179**, 5845–5854 (2007). [doi:10.4049/jimmunol.179.9.5845](https://doi.org/10.4049/jimmunol.179.9.5845) [Medline](#)
 54. S. R. Ferdosi, R. Ewaisha, F. Moghadam, S. Krishna, J. G. Park, M. R. Ebrahimkhani, S. Kiani, K. S. Anderson, Multifunctional CRISPR-Cas9 with engineered immunosilenced human T cell epitopes. *Nat. Commun.* **10**, 1842 (2019). [doi:10.1038/s41467-019-09693-x](https://doi.org/10.1038/s41467-019-09693-x) [Medline](#)
 55. M. Kalos, B. L. Levine, D. L. Porter, S. Katz, S. A. Grupp, A. Bagg, C. H. June, T cells with chimeric antigen receptors have potent antitumor effects and can establish memory in patients with advanced leukemia. *Sci. Transl. Med.* **3**, 95ra73 (2011). [doi:10.1126/scitranslmed.3002842](https://doi.org/10.1126/scitranslmed.3002842) [Medline](#)

ACKNOWLEDGMENTS

We thank the Human Immunology Core at the University of Pennsylvania for providing leukocytes for research, the Clinical Cell and Vaccine Production Facility for GMP cell manufacturing, the Hospital of the University of Pennsylvania Apheresis Unit for peripheral blood mononuclear cell collections from which NYCE T cells were manufactured, regulatory assistance from E. Meagher, S. Emmanuel and E. Veloso and the Office of Clinical Research, the Center for Advanced Retinal and Ocular Therapeutics Clinical Vector Core (CAROT CVC), J. Everett for data analysis with iGUIDE, C. Bartoszek, J. Finklestein, M. Gohil, A. Kim, N. Koterba, M. Mahir, B. Menchel, T. Mikheeva, F. Nazimuddin, H. Parakandi, R. Reynolds and T. Yoder for experimental support, W. Gladney for protocol development and management, and R. Chiarle at the Boston Children's Hospital for helpful discussions. **Funding:** This work was funded by the National Institutes of Health (grant 2R01CA120409 to Y.Z. and C.H.J.), Alliance for Cancer Gene Therapy Investigator's Award (J.A.F., R.M.Y.), NCI P01 CA214278 (J.A.F., R.M.Y., S.F.L. and C.H.J.), NCI U54 CA24711 (J.A.F., M.M.D., R.M.Y. and C.H.J.), NIA U01 AG066100 (J.A.F., R.M.Y. and C.H.J.), NSF Engineering Research Center for Cell Manufacturing Technologies Seed Grant (J.A.F. and B.L.L.), Abramson Cancer Center Emerging Cancer Informatics Center of Excellence Award, (J.A.F.) and sponsored research grants from the Parker Institute for Cancer Immunotherapy and Tmunity Therapeutics. **Author contributions:** Conceptualization: Y.Z., C.H.J., F.D.B. Data curation: V.E.G. Formal Analysis: W-T.H., J.A.F. Funding acquisition: C.H.J. Investigation: E.A.S., A.C., K.L.W., A.D.C., E.L., P.A.M., I.K., M.G., J.X., I-y.J., J.S., T.M., A.C., A.L.G., S.D., A.L., K.R.P., Y.Q., A.T.S., H.Y.C., B.M.C. Methodology: L.T., A.F., J.S.-M., F.D.B. Project administration: R.M.Y., A.C., G.P., J.K.J. Software: C.L.N. Supervision: J.A.F., S.F.L., E.O.H., J.J.M., R.M.Y., D.L.S. Validation: V.G., F.C., L.T., M.M.D., S.F.L., J.S.-M. Writing – original draft: E.A.S., J.A.F., S.F.L., C.H.J. Writing – review and editing: B.L.L., D.L.S., H.Y.C., F.D.B. **Competing interests:** Y.Z. and C.H.J. are inventors on patent applications 15/516,052 and WO2016069282A1 submitted by the University of Pennsylvania, that covers the use of gene modification in T cells for adoptive cell therapy. A.C., B.L.L., Y.Z. and C.H.J. are scientific founders of Tmunity and have equity in Tmunity. J.A.F. and M.M.D. have funding support from Tmunity. A.T.S. is a scientific founder of Immunai and has funding support from Arsenal Biosciences. S.F.L. has funding support from Tmunity, Cabaletta, Novartis, consultant for Gilead/Kite. H.Y.C. is a co-founder of Accent Therapeutics, Boundless Bio, and a consultant of 10x Genomics, Arsenal Biosciences, and Spring Discovery. The other authors declare no competing interests. **Data and materials availability:** iGUIDEseq data have been deposited with links to BioProject accession number PRJNA601142 in the NCBI BioProject database (<https://www.ncbi.nlm.nih.gov/bioproject/>). Single-cell RNA seq data have been deposited into the database of Genotypes and Phenotypes dbGaP (<https://www.ncbi.nlm.nih.gov/gap/>) under accession number phs001707. Reagents are available under an MTA with the University of Pennsylvania; address requests to C.H.J.

SUPPLEMENTARY MATERIALS

science.sciencemag.org/cgi/content/full/science.aba7365/DC1

Materials and Methods

Supplementary Text

Figs. S1 to S10

Tables S1 to S6

References (51–55)

3 January 2020; accepted 28 January 2020
Published online 6 February 2020
10.1126/science.aba7365

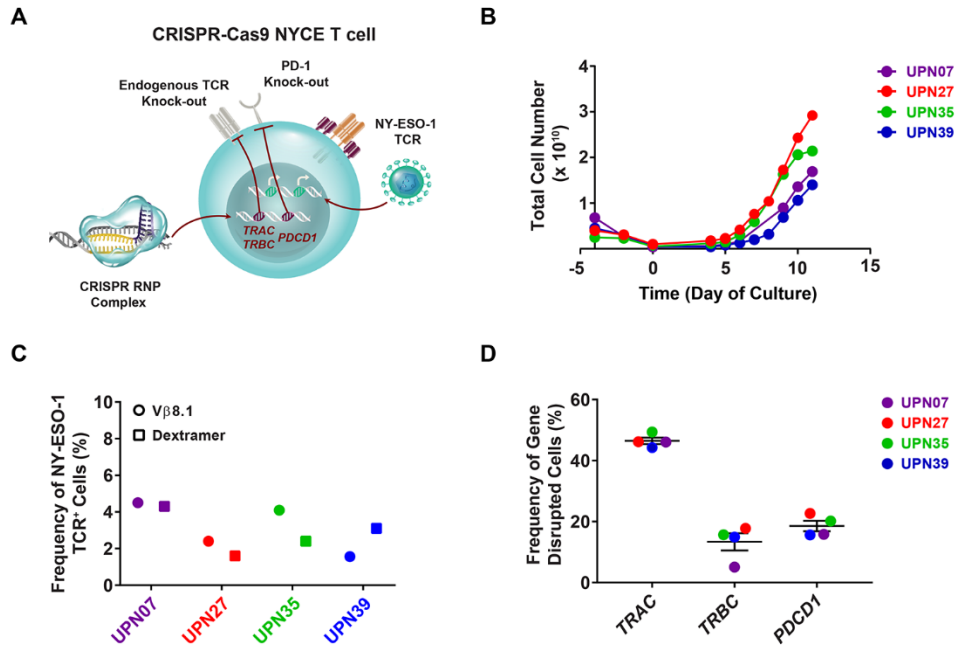


Fig. 1. Feasibility of CRISPR-Cas9 NYCE T cell engineering. (A) Schematic representation of CRISPR-Cas9 NYCE T cells. (B) Large-scale expansion of NYCE T cells. Autologous T cells were transfected with Cas9 protein complexed with single guide RNAs (ribonucleoprotein; RNP complex) against *TRAC*, *TRBC* (i.e., endogenous TCR deletion) and *PDCD1* (i.e., PD-1 deletion) and subsequently transduced with a lentiviral vector to express a transgenic NY-ESO-1 cancer-specific TCR. Cells were expanded in dynamic culture for 8 to 12 days. On the final day of culture, NYCE T cells were harvested and cryopreserved in infusible medium. The total number of enriched T cells during culture is plotted for all four subjects (UPN07, UPN27, UPN35 and UPN39). (C) NY-ESO-1 TCR transduction efficiency was determined in harvested infusion products by flow cytometry. Data are gated on live CD3-expressing and V β 8.1 or dextramer positive lymphocytes and further gated on CD4 and CD8 positive cells. (D) The frequencies of *TRAC*, *TRBC* and *PDCD1* gene-disrupted total cells in NYCE infusion products were measured using chip-based digital PCR. All data are representative of at least two independent experiments. Error bars represent mean \pm SEM.

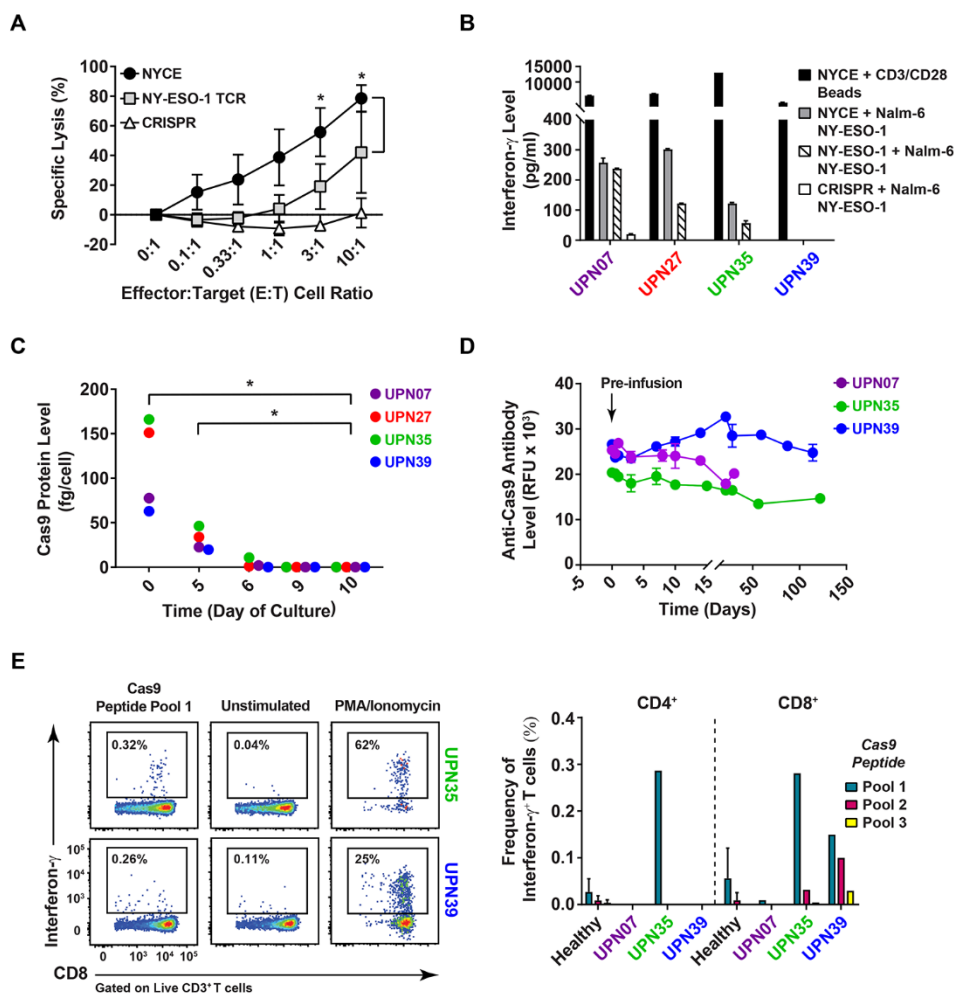


Fig. 2. Potency and immunogenicity of CRISPR-Cas9 engineered T cells. (A) Cytotoxicity of NYCE T cells cocultured with HLA-A*0201 positive Nalm-6 tumor cells engineered to express NY-ESO-1 and luciferase. Patient T cells transduced with the NY-ESO-1 TCR without CRISPR-Cas9 editing (NY-ESO-1 TCR) and untransduced T cells with CRISPR-Cas9 editing of *TRAC*, *TRBC* and *PDCD1* (denoted as here as CRISPR) were included as controls ($n = 4$ patient T cell infusion products). Asterisks indicate statistical significance determined by paired t -tests between groups ($*P < 0.05$). Error bars represent SEM. (B) Levels of soluble interferon- γ produced by patient NYCE T cell infusion products (denoted as NYCE) following a 24-hour co-culture with anti-CD3/CD28 antibody-coated beads or NY-ESO-1-expressing Nalm-6 target cells. Patient NY-ESO-1 TCR transduced T cells (NY-ESO-1 TCR) and untransduced, CRISPR-Cas9 edited T cells (denoted as CRISPR) served as controls. Error bars indicate SEM. (C) Quantification of residual Cas9 protein in NYCE T cell infusion products in clinical-scale manufacturing is shown over time. Asterisks depict statistical significance determined by paired t -tests between time points ($*P < 0.05$). (D) Results from the fluorescence-based indirect ELISA screen performed to detect antibodies against Cas9 protein in the sera of three patients treated with NYCE T cells. Each dot represents the amount of anti-Cas9 signals detected in patient serum prior to T cell infusion (denoted by a vertical black arrow) and at various time points following NYCE T cell transfer. RFU = relative fluorescent units. (E) Immunoreactive Cas9-specific T cells in baseline patient leukapheresis samples were detected. Representative flow cytometry plots (left panel) from two patients whose T cells were positive for interferon- γ in response to Cas9 peptide stimulation. Unstimulated T cells treated with vehicle alone (dimethyl sulfoxide, DMSO) served as a negative control, while matched T cells stimulated with phorbol myristate acetate (denoted as PMA)/ionomycin served as a positive control. Bar graphs (right panel) show the frequency of ex vivo CD4 $^+$ and CD8 $^+$ T cells from patients or healthy donor controls ($n = 6$) that secrete interferon- γ in response to stimulation with three different Cas9 peptide pools. The background frequency of interferon- γ -expressing T cells (unstimulated control group, DMSO alone) is subtracted from the values shown in the bar graph. Error bars depict SD.

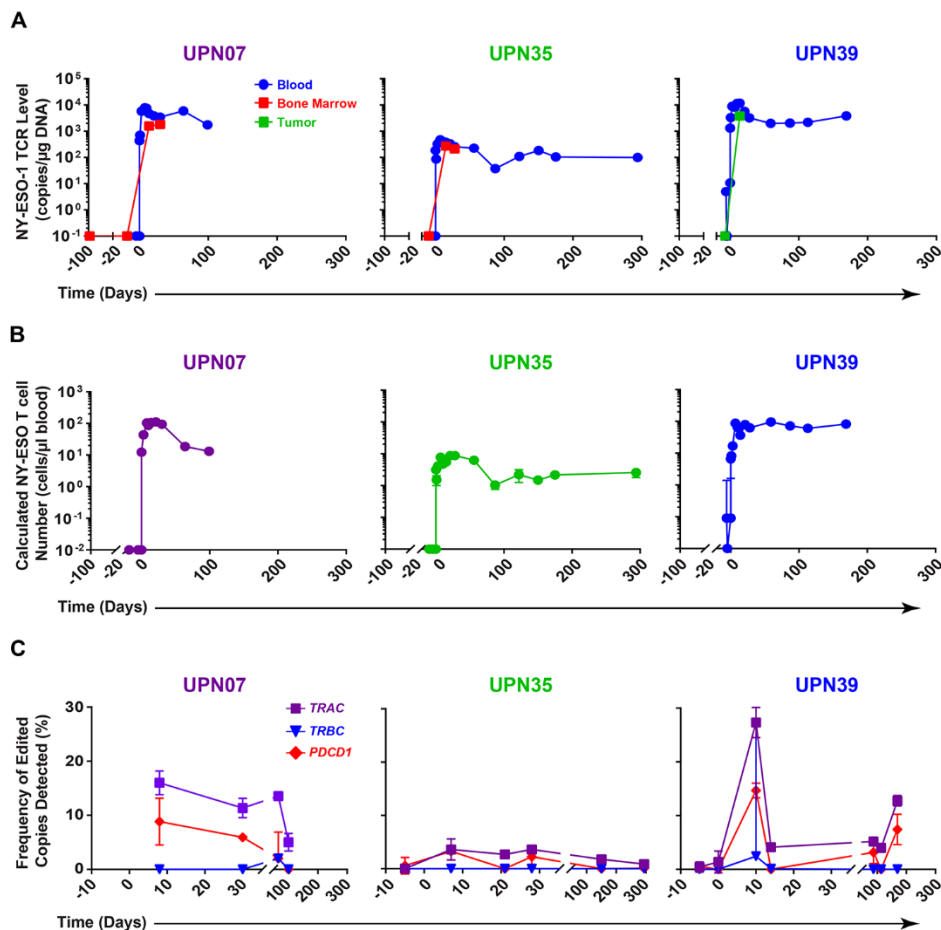


Fig. 3. Sustained in vivo expansion and persistence of CRISPR-Cas9 engineered T cells in patients. (A) The total number of vector copies per microgram of genomic DNA of the NY-ESO-1 TCR transgene in the peripheral blood (UPN07, UPN35 and UPN39), bone marrow (UPN07 and UPN35; multiple myeloma), and tumor (UPN39; sarcoma) is shown pre- and post-NYCE T cell infusion. (B) Calculated absolute numbers of NY-ESO-1 TCR-expressing T cells per microliter of whole blood from the time of infusion to various post-infusion time points in the study are shown. The limit of detection is approximately 2.5 cells/μl of whole blood. (C) Frequencies of CRISPR-Cas9-edited T cells (*TRAC*, *TRBC* and *PDCD1* knockout) before and following adoptive cell transfer are depicted. Error bars indicate SD.

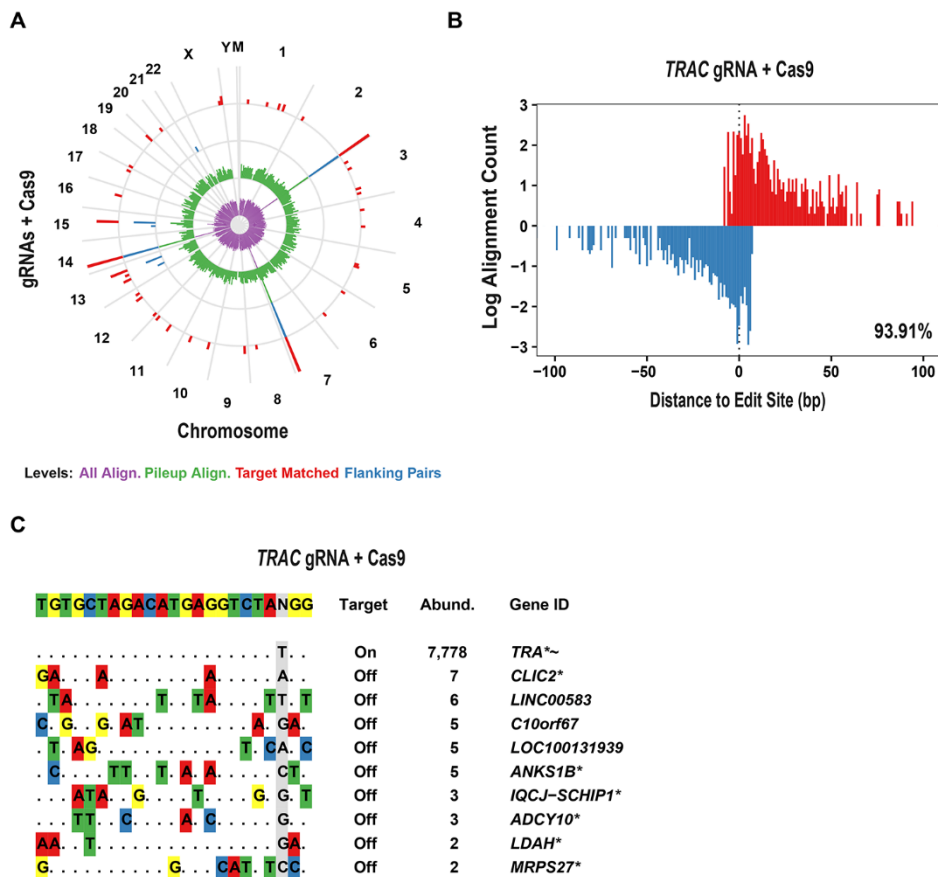


Fig. 4. Fidelity of CRISPR-Cas9 gene editing. (A) Genomic distribution of oligonucleotide (dsODN) incorporation sites, which mark locations of double strand breaks. The ring indicates the human chromosomes aligned end-to-end, plus the mitochondrial chromosome (labeled M). The targeted cleavage sites are on chromosomes 2, 7, and 14. The frequency of cleavage and subsequent dsODN incorporation is shown on a log scale on each ring (pooled over 10 Mb windows). The purple inner most ring plots all alignments identified. The green ring shows “pile ups” of three or more overlapping sequences; the blue ring shows alignments extending along either strand from a common dsODN incorporation site (“flanking pairs”); the red ring shows reads with matches to the gRNA (allowing <6 mismatches) within 100 bp (“target matched”). (B) Distribution of inferred positions of cleavage and dsODN incorporation at an on-target locus. Incorporations in different strand orientations are shown on the positive (red) and negative (blue) y-axis. The percentage in the bottom right corner is an estimate of the number of incorporations associated with the on-target site (based on pileups) captured within the allowed window of 100 bps. (C) Sequences of sites of cleavage and dsODN incorporation are shown, annotated by whether they are on target or off target (“Target”); the total number of unique alignments associated with the site (“Abund”); and an identifier indicating the nearest gene (“Gene ID”). *Symbols after the gene name indicate that the site is within the transcription unit of the specific gene, whereas the ~ symbol indicates the gene appears on the allOnc cancer-associated gene list.

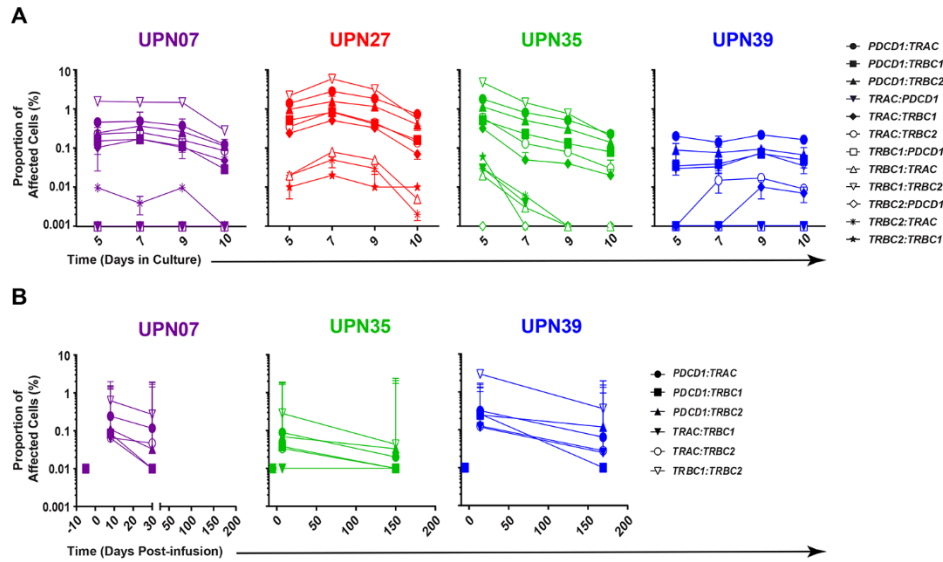


Fig. 5. Detection of chromosomal translocations in engineered T cells following CRISPR-Cas9 gene editing. (A) Evaluation of chromosomal translocations in NYCE T cell infusion products during the course of large-scale culture is shown. For the 12 monocentromeric translocation assays conducted, a positive reference sample that contains 1×10^3 copies of the synthetic template plasmid was evaluated as a control and the percent difference between expected and observed marking was calculated. The absence of amplification from the 12 reactions that correspond to the different chromosomal translocations indicates assay specificity (see supplemental methods). (B) Longitudinal analysis of chromosomal translocations in vivo in three patients pre- and post-NYCE T cell product infusion is displayed. In (A) and (B), error bars denote SD. For graphical purposes, the proportions of affected cells were plotted on a log scale; a value of 0.001% indicates that translocations were not detected.

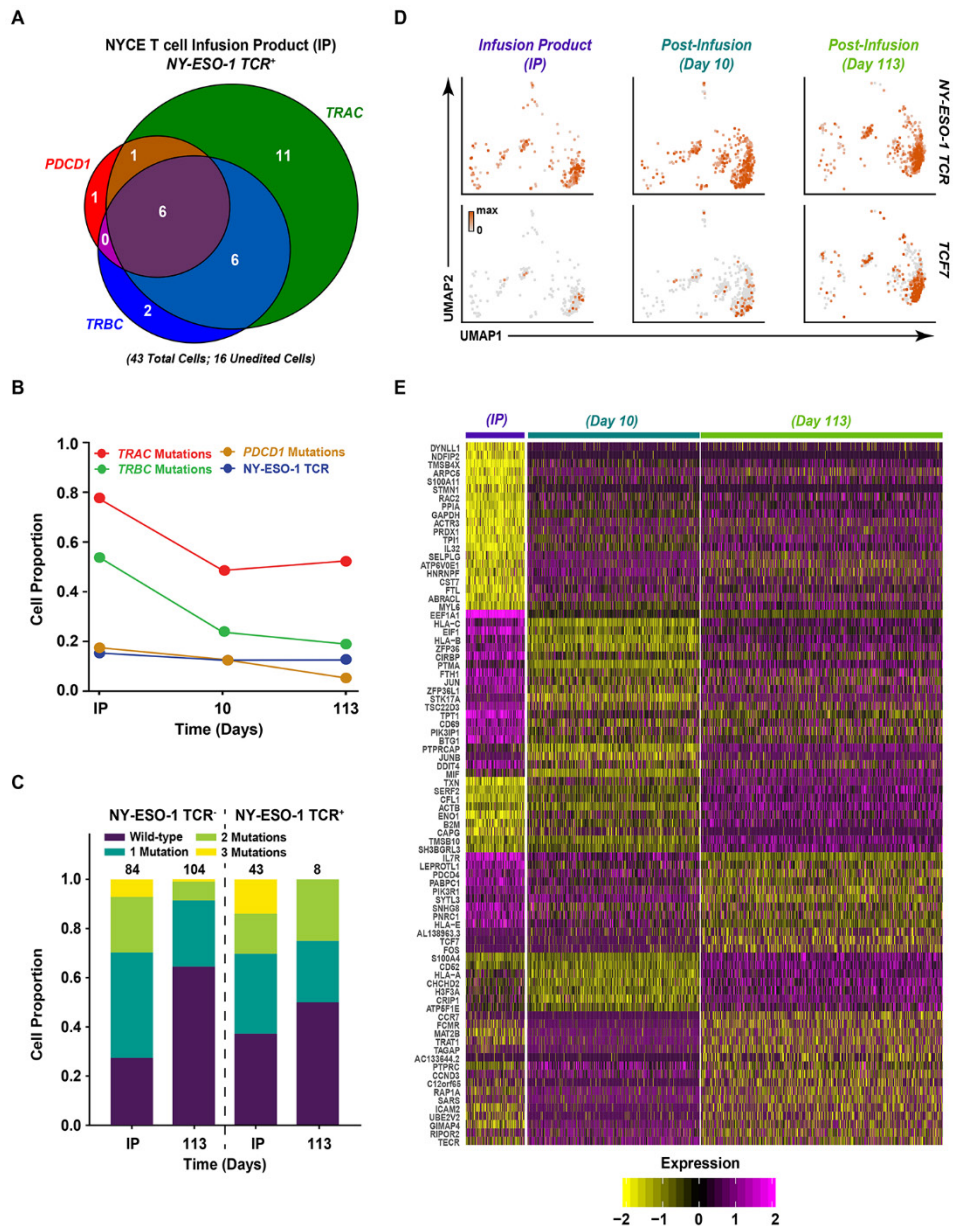


Fig. 6. Single-cell RNA sequencing of patient UPN39 CRISPR-Cas9 engineered NYCE T cells pre- and post-infusion. (A) Venn diagram showing relative numbers of NY-ESO-1 TCR-positive cells with *TRAC*, *TRBC* and/or *PDCD1* mutations in the NYCE T cell infusion product (Day 0). (B) Proportions of pre-infusion (Day 0) and post-infusion (Days 10 and 113) T cells without mutations (wild-type), with *TRAC*, *TRBC*, *PDCD1* mutations or expressing the NY-ESO-1 TCR transgene. Numbers of cells belonging to each of these categories are listed below the graph. (C) Analysis of NY-ESO-1 TCR-positive (right) and TCR-negative (left) cells without mutations (wild-type) or with single, double or triple mutations at Day 0 (NYCE T cell infusion product) and Day 113 post-NYCE T cell infusion. (D) UMAP plots of gene expression data. Analysis was performed on all T cells integrated across time points, but only NY-ESO-1 TCR-expressing cells, split by time point, are shown (top panel). The increase in *TCF7* expression is indicative of an acquired central memory phenotype (bottom panel, same cells). (E) Heat map showing scaled expression of differentially expressed genes in NY-ESO-1 TCR-positive T cells across time points. Color scheme is based on scaled gene expression from -2 (yellow) to 2 (purple).

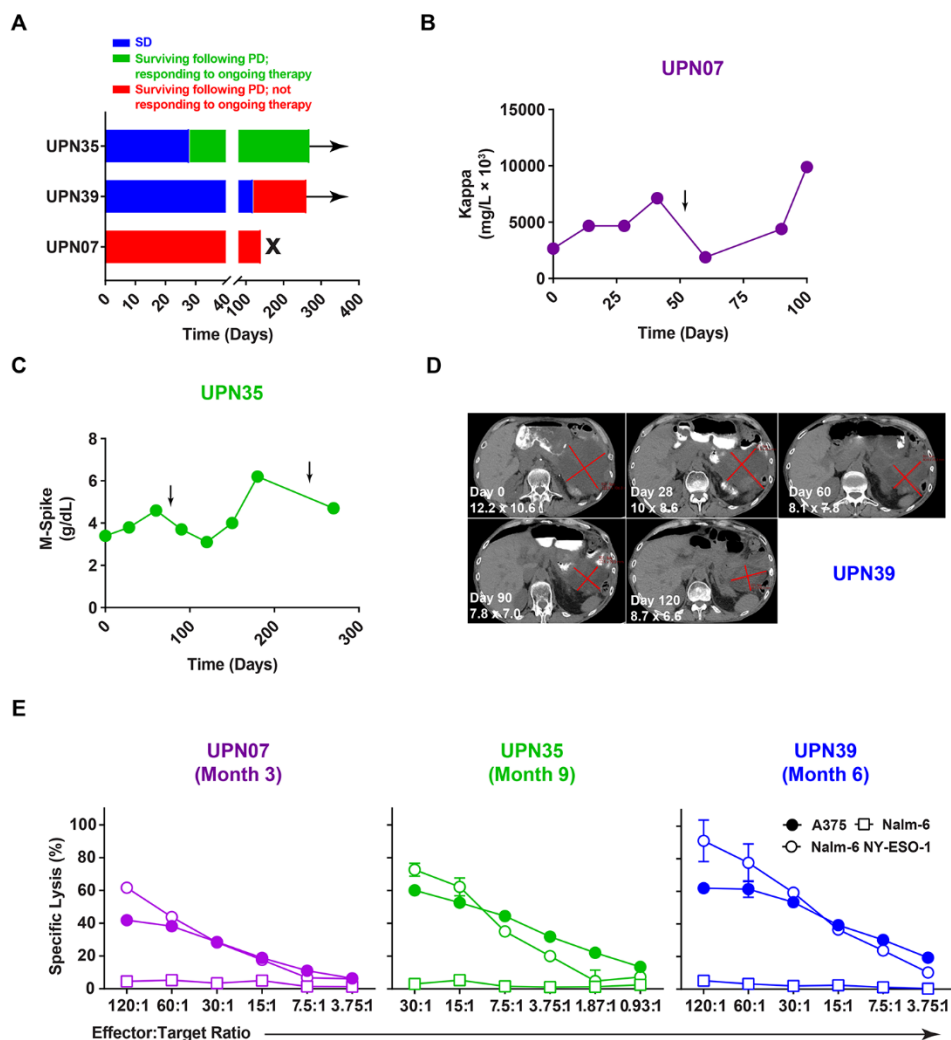


Fig. 7. Clinical responses and patient outcome following infusion of CRISPR-Cas9 engineered NYCE T cells. (A) Swimmer's plot describing time on study for each patient, duration of follow-up off study (defined as survival beyond progression or initiation of other cancer therapy) and present status (differentially colored) is shown. Arrows indicate ongoing survival. (B) Changes in kappa light chain levels (mg/L × 10³) in patient UPN07 following NYCE T cell product infusion are depicted. Vertical black arrow indicates initiation of a D-ACE salvage chemotherapy regimen (defined as intravenous infusion of cisplatin, etoposide, cytarabine and dexamethasone). (C) Longitudinal M-Spike levels (g/dL) in patient UPN35 post-NYCE T cell product administration are shown. Vertical black arrows denote administration of combination therapy with elotuzumab, pomalidomide and dexamethasone. (D) Computed tomography scans demonstrating tumor regression in patient UPN39 following administration of an autologous NYCE T cell infusion product. Radiologic studies were obtained before therapy and after adoptive transfer of NYCE T cells. Tumor is indicated by red X. SD, stable disease; PD, progressive disease. (E) Cytolytic capacity of NY-ESO-1-specific CD8⁺ T cells recovered at the indicated month after infusion and expanded from patients is shown. PBMC samples collected after NYCE T cell product infusion were expanded in vitro in the presence of NY-ESO-1 peptide and IL-2. The ability of expanded effector cells to recognize antigen and elicit cytotoxicity was tested in a 4-hour ⁵¹CR release assay incorporating Nalm-6 NY-ESO-1⁺, parental Nalm-6 (NY-ESO-1⁻) and A375 melanoma cells (NY-ESO-1⁺). All target cell lines were HLA-A*02 positive. Assays were performed in triplicate and error bars represent SD.

Table 1. Patient demographics and date of engineered T cell infusion. UPN, unique patient number; MM, multiple myeloma; BM, bone marrow; XRT, radiation therapy; ASCT, autologous hematopoietic stem cell transplant; ND, not done.

Subject ID (UPN) / Infusion date	Gender / Age	Diagnosis	Clinical Sites	Prior Therapy	Prior Transplant / Surgery	LAGE-1* / NY-ESO-1* / NY-ESO-1**
UPN35 1/7/19	Female / 66 years	IgG kappa MM 2008	BM, lytic bone lesions	Lenalidomide, pomalidomide, bortezomib, carfilzomib, daratumumab, panobinostat (8 lines; see supplementary materials)	ASCT x 3	Pos/Pos/Neg
UPN39 3/18/19	Male / 66 years	Myxoid/ round cell liposarcoma 2012	Abdominal/ pelvic masses	Doxorubicin, ifosfamide, XRT 60-Gy, trabectedin, gemcitabine, taxol, XRT	Resection/ debulking x 2, left nephrec- tomy/ partial sigmoid resection	ND/ND/Pos
UPN07 8/5/19	Female / 62 years	Kappa light chain MM 2009	BM, lytic bone lesions	Lenalidomide, pomalidomide, bortezomib, carfilzomib, daratumumab, anti-CD38 immunoconjugate (6 lines; see supplementary materials)	ASCT x 2	Pos/Pos/Neg

*qPCR

**Immunohistochemistry

Table 2. List of adverse events on the study.

AE Category	Toxicity	All Grades	Grade 1/2	Grade 3/4
Hematologic	Anemia	2	1	1
	Leukopenia	4	-	4
	Neutropenia	4	1	3
	Thrombocytopenia	6	3	3
	Lymphopenia	1	-	1
Infection	Upper Respiratory	1	1	-
	Febrile Neutropenia	2	-	2
Electrolyte	Hypercalcemia	1	1	-
	Hyperphosphatemia	1	1	-
	Hypoalbuminemia	1	1	-
	Hypocalcemia	3	2	1
	Hypokalemia	1	1	-
	Hypomagnesemia	1	1	-
	Hyponatremia	1	1	-
	Hypophosphatemia	1	-	1
Neurologic	Dysgeusia	1	1	-
	Headache	1	1	-
	Paresthesia	2	2	-
	Syncope	1	-	1
	Pain	3	3	-
Renal	Acute kidney injury	1	1	-
	Urinary obstruction	1	-	1
Respiratory	Aspiration	1	-	1
	Nasal congestion	1	1	-
	Cough	2	2	-
Gastrointestinal	Lower GI bleed	1	1	-
	Vomiting	1	1	-
Other	Alopecia	1	1	-
	Phlebitis	1	1	-
	LE edema	1	1	-
Total		50	30	20

Table 3. iGUIDE measurement of on-target editing efficiency for each gene by final product.

Manufactured NYCE T cell Product (Subject ID)	<i>PDCD1</i>	<i>TRAC</i>	<i>TRBC</i>
UPN07	100.0%	99.6%	96.1%
UPN27	99.6%	99.1%	96.8%
UPN35	99.8%	99.1%	97.0%
UPN39	98.2%	96.7%	93.5%
Average ± SD	99.4% ± 0.8%	98.6% ± 1.3%	95.8% ± 1.6%

CRISPR-engineered T cells in patients with refractory cancer

Edward A. Stadtmauer, Joseph A. Fraietta, Megan M. Davis, Adam D. Cohen, Kristy L. Weber, Eric Lancaster, Patricia A. Mangan, Irina Kulikovskaya, Minnal Gupta, Fang Chen, Lifeng Tian, Vanessa E. Gonzalez, Jun Xu, In-young Jung, J. Joseph Melenhorst, Gabriela Plesa, Joanne Shea, Tina Matlawski, Amanda Cervini, Avery L. Gaymon, Stephanie Desjardins, Anne Lamontagne, January Salas-McKee, Andrew Fesnak, Donald L. Siegel, Bruce L. Levine, Julie K. Jadowsky, Regina M. Young, Anne Chew, Wei-Ting Hwang, Elizabeth O. Hexner, Beatriz M. Carreno, Christopher L. Nobles, Frederic D. Bushman, Kevin R. Parker, Yanyan Qi, Ansuman T. Satpathy, Howard Y. Chang, Yangbing Zhao, Simon F. Lacey and Carl H. June

published online February 6, 2020

ARTICLE TOOLS

<http://science.sciencemag.org/content/early/2020/02/05/science.aba7365>

SUPPLEMENTARY MATERIALS

<http://science.sciencemag.org/content/suppl/2020/02/05/science.aba7365.DC1>

RELATED CONTENT

<http://science.sciencemag.org/content/sci/367/6478/616.full>
<http://science.sciencemag.org/content/sci/early/2020/02/05/science.aba9844.full>

REFERENCES

This article cites 55 articles, 20 of which you can access for free
<http://science.sciencemag.org/content/early/2020/02/05/science.aba7365#BIBL>

PERMISSIONS

<http://www.sciencemag.org/help/reprints-and-permissions>

Use of this article is subject to the [Terms of Service](#)

Science (print ISSN 0036-8075; online ISSN 1095-9203) is published by the American Association for the Advancement of Science, 1200 New York Avenue NW, Washington, DC 20005. The title *Science* is a registered trademark of AAAS.

Copyright © 2020, American Association for the Advancement of Science